

Calculation of the Ionization Potentials and Electron Affinities of Bacteriochlorophyll and Bacteriopheophytin via *ab Initio* Quantum Chemistry

Joseph Crystal and Richard A. Friesner*

Columbia University, New York, New York 10027

Received: April 22, 1999; In Final Form: September 13, 1999

Ionization potentials (IP) and electron affinities (EA) are calculated for bacteriopheophytin (BPh) and bacteriochlorophyll (BChl) in the photosynthetic reaction center utilizing density functional methods implemented in a parallel version of the JAGUAR electronic structure code. These quantities are studied as a function of basis set size and molecular geometry. The results indicate the necessity of using large basis sets with diffuse functions in order to obtain reliable IP and EA in the gas phase. The relative reduction potentials of BChl and BPh in dimethylformamide solution are also calculated and compared with experimental results. Excellent agreement between theory and experiment is obtained when ligand binding of solvent molecules to the central Mg atom of BChl is incorporated in the calculations.

I. Introduction

Electron-transfer reactions are at the heart of many central biochemical processes, including the reactions occurring in the photosynthetic reaction center (RC). Most electron-transfer reactions involve specialized chromophores associated with the relevant proteins. In the case of the bacterial RC, the molecules involved are bacteriochlorophyll (BChl) and bacteriopheophytin (BPh), which differ only by the presence or absence of a magnesium center, respectively. Knowledge of the redox potentials—the ionization potential and electron affinity—of the various chromophores in the protein environment is therefore fundamental in understanding the electron-transfer mechanism, as well as in calculating electron-transfer thermodynamics and kinetics quantitatively.

To compare the calculated redox potentials with experimental values, one would like to reliably calculate the redox potentials to an accuracy on the order of 0.1 eV (2.3 kcal/mol) or better. However, achieving the desired accuracy poses several challenges. First, fundamental quantum chemical computations are required to determine the gas-phase ionization potential (IP) or electron affinity (EA). The effects of the protein environment, including solvation, must then be taken into account. Finally, there are issues concerning conformational sampling, although these issues are actually less critical for the RC, as the system appears to be unusually rigid and functions well at liquid helium temperatures. Each of these aspects of the problem poses a formidable computational challenge.

Over the past decade, there have been numerous attempts to calculate chromophore redox potentials for a variety of systems, including many studies that have focused on the RC.^{1–3} In the latter case, a very wide range of values has been obtained, corresponding to the different approaches used to address the problems described above. While some of these calculations have obtained results close to the experimental values, the results have typically been dependent upon a number of ad hoc assumptions, and it is clear that a reliable methodology has not yet been developed. Indeed, at the present time, none of the individual components of the calculations can be said to be robustly converged to a reasonable level.

The objective of our research program in this area is to improve each aspect of the computational methodology systematically until the errors obtained lie within well-controlled limits. In this paper, this process is begun by determining the level of calculation necessary to produce reliable gas-phase ionization potentials for BChl and BPh via *ab initio* quantum chemical methods, i.e., hybrid density functional (DFT) methods^{4–6} with large basis sets. Recent work by Blomberg et al.¹⁹ has addressed this problem with DFT methods, but the calculations were restricted to relatively small basis double- ζ (DZ) basis sets. In contrast, we obtain results for basis sets as large as augmented triple- ζ , which appear to be sufficient to converge the DFT results.

The paper is organized as follows. In section II, the quantum chemical computational methods are briefly described. Section III presents results for the ionization potentials of BChl and BPh, examining the convergence of energy differences with basis set size and as a function of geometry. The ionization potentials and electron affinities of BChl and BPh are also investigated in the presence of the solvent dimethylformamide (DMF), initially using a continuum dielectric approach to model the solvation effects. For BChl, the continuum description is then augmented by considering the liganding of a solvent molecule to the central Mg atom. These results are then compared to the experimental results of Fajer and co-workers.⁷ Finally, future directions are discussed in section IV.

II. Computational Methods

Ab initio DFT calculations are carried out using the Jaguar suite of electronic structure programs.⁸ The B3LYP hybrid density functional^{4–6} was used to obtain all results reported below. The average error in ionization energies and electron affinities for the G2 set of small molecule test cases⁹ is 2 kcal/mol, a value that is approximately within our accuracy criteria for the redox potential calculation. It must be pointed out that there is no guarantee that the results obtained for the small molecule test cases will apply equally well to a large, complex

ring system such as a porphyrin. However, given the impressive transferability of error to large systems that DFT methods have demonstrated over the past five years, it would not be surprising if the resultant errors were within the above limits, provided that the basis set is suitably converged.

A series of basis sets of increasing size (and quality) are employed to investigate basis set convergence. The largest calculations carried out require on the order of 2000 basis functions. These large calculations are intractable with Gaussian 94 owing to overcompleteness of the basis set, according to reports in ref 19. Jaguar avoids this problem by projecting the basis vectors with small eigenvalues in the overlap matrix out of the active space, thereby allowing stable results to be obtained in a routine fashion. Jaguar's computational efficiency for DFT calculations¹⁰ has also been critical in carrying out the calculations in a reasonable amount of time.

To further reduce the computational time, a parallel version of Jaguar, using an MPI implementation and running on either an IBM SP2 at Columbia or an SGI Origin 2000 at NCSA, was employed. Parallel calculations were run on four nodes of either machine, which for the system sizes studied leads to a parallel efficiency of 80–90%. Using the parallel code, systems of up to two to three times the size of the systems currently studied could be investigated by increasing the number of nodes on which the computations are run.

Solvation effects are treated via a self-consistent reaction field (SCRF) approach, combining accurate numerical solutions of the Poisson–Boltzmann equation with correlated *ab initio* quantum chemistry. The details of this methodology have been described elsewhere.^{11–13} In SCRF calculations the absolute accuracy of the results is critically dependent upon the dielectric radii assigned to various atoms, and these in turn depend on the nature of the solvent. In addition to the solvent dielectric constant, which is incorporated in the SCRF model, first-shell hydrogen-bonding interactions between solvent and solute must also be accounted for. The dielectric radii in our model have only been optimized for aqueous solvation;¹³ the absolute solution-phase redox potentials are therefore expected to be no better than semiquantitative. However, the relative redox potentials of BPh and BChl may still be expected to achieve a reasonable degree of accuracy.

III. Results

A. Physical Model. The calculations treat the complete BChl (or BPh) molecule with the exception of the phytol tail, which is truncated to save computational effort. The actual structures studied are shown in Figure 1. Truncating the tail is not expected to have any significant effect on the results presented below.

The crystal structures of BChl and BPh were not available for each molecule as an isolated system. Consequently, initial geometries were taken from the Brookhaven data bank, using the X-ray coordinates from the RC structure of Diefenhofer, Michl, and co-workers.^{14,15} The effects of geometry optimization on the ionization potentials and electron affinities were then investigated. Comparison of the energetics obtained from these various optimized geometries, along with structural differences, are presented below.

B. Basis Set Dependence of the Ionization Potential and Electron Affinity. The conventional wisdom regarding DFT calculations, emphasized by Becke, Pople, and others,^{16,17} is that basis sets of at least triple- ζ quality, augmented with diffuse functions, are needed to converge properties such as the ionization potential (IP) and electron affinity (EA). The basis

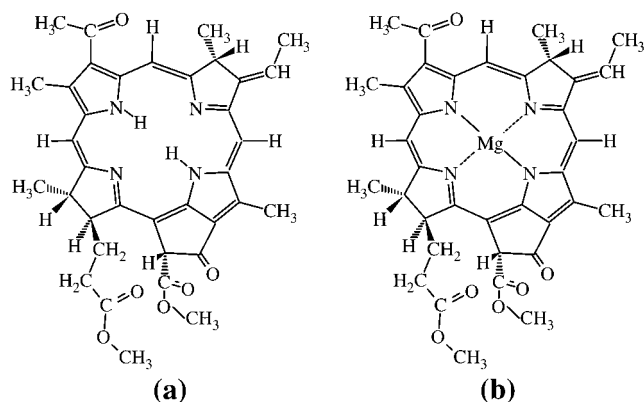


Figure 1. (a) Bacteriopheophytin. (b) Bacteriochlorophyll, with phytol tails removed, used in the calculations.

set requirements are not nearly as large as they are for wave-function-based quantum chemical methods such as CCSD(T),¹⁸ which require large numbers of high angular momentum functions, but they are nevertheless nontrivial. The reason DFT methods are able to yield good results for ionization potentials and electron affinities using smaller basis sets than conventional quantum chemical methods is that the exchange-correlation functional has in effect been parametrized to incorporate some components of the dynamic correlation that do not have to appear in the wave function explicitly. This is particularly the case for higher angular momentum functions, which are primarily needed to resolve the electron–electron cusp at close approach of an electron pair.

Recently, Blomberg and co-workers¹⁹ asserted that the ionization potentials of BChl and BPh converge to high accuracy at the DZ level, using the Dunning cc-pVDZ basis set. Their evidence for this assertion was a small energy difference between a DZ and a DZP calculation; they were unable, however, to carry out any investigations with larger basis sets. Clearly, explicit studies are required to determine whether the cancellation of basis set effects proposed in ref 19 actually occurs. To this end, the following basis sets have been investigated: (1) 6-31G at the DZ level; (2) Dunning cc-pVDZ basis set at the DZ level; (3) 6-31G** at the DZP level; (4) cc-pVTZ (-f) at the TZ2P level; (5) cc-pVTZ and cc-pVTZ++ (-f). The final two basis sets were investigated in order to examine the effects of adding f functions and diffuse functions. Systematic studies of a single geometry then indicate which basis set yields converged results, and this approach is used as the standard for the remaining calculations.

Table 1 presents results for BPh (prior to geometry optimization) using the basis sets described above. Both the ionization potential and electron affinity are computed. It can be seen that convergence of the absolute ionization potential or electron affinity clearly requires the use of a high-quality TZ2P basis set augmented with diffuse functions; f functions have a negligible effect. It is also interesting that the 6-31G and 6-31G** results are very similar. This similarity suggests that the larger basis sets primarily improve the results via the presence of basis functions with small exponents, which provide a better description of the tails of the wave function (in contrast to the tight d polarization functions added to 6-31G to produce the 6-31G** basis). This idea is qualitatively confirmed by the Dunning DZ results, which are between the triple- ζ Dunning basis sets and the 6-31G basis set. The Dunning DZ basis set is more highly contracted than the 6-31G basis set and provides a better description of the long-range part of the wave function,

TABLE 1: Basis Set Dependence for Ionization Potentials and Electron Affinities for Bph (kcal/mol)

| basis set | 6-31G | cc-pVDZ | 6-31G** | cc-pVTZ ^a | cc-pVTZ(-f) | cc-pVTZ(-f)++ |
|---------------|--------|---------|---------|----------------------|-------------|---------------|
| no. basis fns | 490 | 490 | 880 | 1400 | 1777 | 1966 |
| EA | 40.39 | 44.23 | 40.37 | 47.50 | 47.51 | 49.65 |
| IP | 140.71 | 144.40 | 138.87 | 143.74 | 143.75 | 144.95 |

^a Outermost H atoms are 6-31G**.

TABLE 2: Ionization Potentials and Electron Affinities before and after Geometry Optimization (kcal/mol) Using cc-pVTZ(-f)++ Basis

| species | before | | | after | | |
|---------|--------|--------|---------|--------|--------|---------|
| | BPh | BChl-I | BChl-SP | BPh | BChl-I | BChl-SP |
| EA | 49.65 | 50.07 | 48.32 | 49.10 | 51.72 | 51.09 |
| IP | 144.95 | 143.80 | 142.26 | 145.39 | 140.82 | 139.11 |

thus providing a balanced calculation of the electron affinity as compared to the ionization potential. However, this basis set is still not quantitatively converged for the ionization potential or the electron affinity, and the energy difference between these two quantities, the relevant energy when considering the difference in energy between two neutral porphyrins and a state in which charge is separated between the two porphyrins, is similarly not converged, as the major changes in the electron affinity with the increasing size of the basis set indicate. Therefore, our results reveal some quantitative disagreement with the hypothesis put forward in ref 19. The consequences of this discrepancy for the calculation of the charge separation in the RC will be the subject of a subsequent publication.

C. Dependence of the Ionization Potential and Electron Affinity on Geometry. The initial geometries were then optimized with the 6-31G* basis set using B3LYP hybrid density functional theory.^{4–6} The IP's and EA's for the optimized geometries are presented in Table 2. Several interesting trends are immediately observed. The ionization potentials for the BChl-I and BChl-SP are closer after optimization, but still not identical. Changes on the order of 0.5–3 kcal/mol are observed upon structural optimization. Although this change is not extremely large, it is nontrivial considering that a change of this magnitude in the energy gap between the primary donor and intermediate acceptor states could result in a 10–20 times larger change on the observed rate of primary charge separation in the RC. The question as to whether the geometrical differences manifested in the crystal structure (and corresponding differences in IP and EA reported here) are actually present in the RC (the issue here is the precision of the crystal structure for the details of the porphyrin geometry) can be further addressed with quantum chemical methods via QM/MM techniques in which the chromophores are optimized in the RC environment. This will be the subject of a subsequent paper.

To further test whether the optimized geometries obtained for BPh and BChl are a unique lowest energy conformation, we took the BPh and BChl-I optimized geometries and swapped the Mg atom between them (thus converting the BPh to a BChl and the BChl to a BPh). These structures were then subjected to a new round of geometry optimization. The results, presented in Table 3, indicate that good agreement is obtained for the IP and EA with the initially optimized structures of each moiety. This result suggests that the optimized structures of BChl and BPh that we have obtained here are reasonable representations of the geometry in a more or less uniform environment, e.g., in solution, which is relevant to our next series of calculations.

D. Estimation of the Electron Affinity of BChl and BPh in Solution. Tables 4 and 5 present solvation energies for BChl and BPh in the solvent DMF for the geometries presented in

TABLE 3: Ionization Potentials and Electron Affinities before and after Second Round of Geometry Optimization (kcal/mol)

| species | before | | after | |
|---------|--------|--------|--------|--------|
| | BPh | BChl | BPh | BChl |
| EA | 49.10 | 51.72 | 50.19 | 51.41 |
| IP | 145.39 | 140.82 | 144.72 | 140.95 |

TABLE 4: Solvation Energies before Geometry Optimizations (kcal/mol) Using 6-31G Basis**

| | Bph | BChl-I | BChl-SP |
|---------|--------|--------|---------|
| anion | −45.99 | −51.04 | −51.70 |
| neutral | −16.51 | −23.66 | −22.08 |
| cation | −47.19 | −55.05 | −51.97 |

TABLE 5: Solvation Energies after Geometry Optimization (kcal/mol) Using 6-31G Basis**

| | Bph | BChl-I | BChl-SP |
|---------|--------|--------|---------|
| anion | −44.09 | −48.11 | −48.92 |
| neutral | −13.76 | −20.21 | −21.05 |
| cation | −43.06 | −50.74 | −50.12 |

TABLE 6: Comparison of Reduction Potentials with Experiment (kcal/mol)

| | HF ²⁰ (no optimization) | DFT (before optimization) | DFT (after optimization) | experiment ⁷ |
|------------------|------------------------------------|---------------------------|--------------------------|-------------------------|
| BPh | 61.22 | 79.13 | 79.43 | 92.24 |
| BChl-I | 59.84 | 77.45 | 79.62 | 87.63 |
| BChl-SP | 61.76 | 77.94 | 78.96 | na ^a |
| diff(BPh−BChl-I) | 1.38 | 1.68 | −0.19 | 4.61 |

^a Not available.

Table 2. As in ref 20, the solvent is modeled via an SCRf model with DMF having a dielectric constant of 36.7 and a probe radius of 2.67 Å using the 6-31G** basis set. The total energy is given by the sum of the gas-phase energy and the solvation energy. The resulting reduction potentials are presented in Table 6. As the results clearly indicate, employing the DFT calculations with a large basis set for the gas-phase energetics yields a significant improvement in the absolute redox energies (obtained from the experimental data in ref 7 as discussed in ref 20) as compared to the small basis set Hartree–Fock calculations of ref 20, with the deviation from experiment diminishing from ~30 to ~10 kcal/mol. The remaining discrepancy can most likely be attributed to the fact that the dielectric radii of the solute functional groups have not been optimized for the DMF solvent—a highly nontrivial task. The improved absolute redox energies are certainly encouraging.

The relative redox energies, however, as presented in Table 6, are very similar to those computed at the HF/6-31G** level before geometry optimization, and the result diverges from the experimental results after optimization. While there are minor fluctuations in the results, it appears that if one employs consistent geometries for both species there is little difference in either the gas-phase or solution-phase redox potentials (on the order of 1 kcal/mol). The BChl and BPh energies before optimization yield a difference in redox potential of 1.68 kcal/

TABLE 7: Binding Energies for DMF to BChl-I (kcal/mol)

| BChl-I | binding energy |
|------------|----------------|
| neutral | 18.13 |
| anion | 11.21 |
| difference | 6.92 |

mol, while the optimized geometries yield a difference of less than 1 kcal/mol. Clearly both results lie outside the range of the experimental result for the differential redox potential of 4.7 kcal/mol.

The apparent insensitivity of this differential to electronic structure method suggests that the difference in redox potentials is due to an effect that is not being properly treated in the SCRF model. The obvious candidate for this discrepancy is the ligand binding of a DMF solvent molecule to the Mg atom in BChl (there is of course no analogous structure for BPh). This binding was hypothesized to cause large errors in the continuum model employed in the present calculation. To test this hypothesis, BChl was reoptimized with one DMF molecule within ligand-binding distance to the Mg atom. During the course of the optimization, there was no significant change in the position of the Mg atom relative to the porphyrin ring. The dielectric continuum model was then used to calculate the solvation free energy of the BChl-DMF complex in both the neutral and reduced states. The idea here is that the continuum description of solvation is a reasonable one for the solvated complex and that any errors in the description will roughly cancel between the neutral and reduced forms. In this approach, the process of forming either a neutral or reduced BChl complex in solution is written as



The difference in total free energy between the neutral and reduced forms can then be written as

$$\Delta G_{\text{redox}}(1) = [(\text{BChl-DMF})](1) - [(\text{BChl}^{(-)}\text{-DMF})](1) \quad (2)$$

where the brackets indicate the total solution-phase energy in a SCRF model, defined as the gas-phase energy plus the solvation free energy. This equation is readily obtained by subtracting the neutral and reduced forms of eq 1, whereupon the solvation free energy of DMF in DMF cancels from both equations.

Before computing the reduction potential via eq 2, we first calculate the binding energy of a DMF molecule to a neutral and a reduced BChl molecule. These values are presented in Table 7. The substantial values of the binding energy suggest that the complexed form is the dominant species in solution, as we hypothesize here. The binding energy in the gas phase of DMF to the neutral form is 6.92 kcal/mol larger than for the ionic form. We conjecture that this is a simple consequence of some negative charge on the ion (which is mostly distributed into the porphyrin ring) leaking into the central Mg atom, thus inhibiting binding to the partial negative charge on the relevant ligand atom.

We now proceed to compute the solvation free energy of the two complexes and determine the corrected reduction potential of BChl and compare the corrected reduction potential with that for BPh. The final result of the calculation puts the relative BChl and BPh redox potentials in DMF into quantitative agreement with experiment (within 0.5 kcal/mol), as shown in Table 8, with the optimized geometry yielding the more accurate results, as expected. The difference in redox potential is thus attributable primarily to ligand binding to the Mg atom as suggested above.

TABLE 8: Reduction Potentials Including Binding Energy (kcal/mol) Compared with Experiment

| species | before geom. optimization | using optimized complex | experiment ⁷ |
|------------|---------------------------|-------------------------|-------------------------|
| BPh | 79.13 | 79.43 | 92.24 |
| BChl-I | 77.45 | 74.93 | 87.63 |
| difference | 1.68 | 4.50 | 4.61 |

This insight will be useful in understanding the relative redox potentials in the RC and in other such problems.

IV. Conclusion

Using parallel DFT calculations with large basis sets, high-quality results for the redox potentials of the neutral, oxidized, and reduced states of the chromophores BChl and BPh have been obtained. While one cannot be completely confident of the ability of the B3LYP density functional to yield accurate results, there is nothing about the calculations to suggest that the errors should not be comparable to those observed for this methodology in studies on the extended G2 database⁹ (± 2 kcal/mol). To our knowledge, these are the largest systems for which redox potentials of this quality have been computed to date. The results presented indicate that if one desires accurate values, it is critical to use large basis sets, with long-range functions assuming the greatest importance. Fortunately, modern electronic structure technology is now capable of handling such calculations on a routine basis.

We believe that to obtain reliable results in the condensed phase it is necessary to bring every component of the calculation up to the level of the present gas-phase energy evaluations. The program to be followed for accomplishing the desired goal is as follows:

(1) Implementation of a mixed quantum mechanical/molecular mechanics (QM/MM) methodology, which will allow rigorous treatment of the interaction of the environment with the chromophores.

(2) Use of an explicitly polarizable force field for the protein, as opposed to a single dielectric constant. This avoids the use of any sort of adjustable parametrization in modeling the protein electrostatic response. Recent work in our group in this area suggests that such a model can be constructed with very high accuracy in modeling the polarization response of the protein.

(3) Inclusion of the entire protein in the calculation (made possible by the QM/MM methodology); treatment of the membrane and water environments by SCRF methods.

(4) Structural optimization of the chromophores with the above features in place.

While these calculations will require a significant amount of CPU time, the dominant contribution will still be the quantum chemistry, and the results presented here demonstrate that this task is clearly tractable with current hardware and software. There is cause for genuine optimism that calculations performed with the above features will result in a truly first-principles prediction of the redox potentials of BChl and BPh in the reaction center environment. If this can be accomplished, it will go a long way toward definitively settling the issue of the mechanism of primary charge separation.

Acknowledgment. This work was supported by the Department of Energy under Grant DE-FG02-90ER14162. Computation time was obtained at NCSA via the NPACI program supported by the National Science Foundation.

References and Notes

- (1) Hansen, L. K. *Photochem. Photobiol.* **1988**, *47*, 903.
- (2) Bixon, M.; Jortner, J.; Michl-Beyerle, M. E. *Biochim. Biophys. Acta* **1991**, *1056*, 301.
- (3) Thompson, M. A.; Zerner, M. C. *J. Am. Chem. Soc.* **1991**, *113*, 8210.
- (4) Becke, A. D. *Phys. Rev. A* **1988**, *38*, 3098.
- (5) Becke, A. D. *J. Chem. Phys.* **1993**, *98*, 5648.
- (6) Lee, C.; Yang, W.; Parr, R. G. *Phys. Rev. B* **1988**, *37*, 785.
- (7) Fajer, J.; Davis, M. S.; Brune, D. C.; Spaulding, L.; Borg, D.; Forman, A. *Brookhaven Symp. Biol.* **1976**, *28*, 74.
- (8) *Jaguar 3.5*; Schrodinger Inc.: Portland, OR, 1998.
- (9) Curtiss, L. A.; Raghavachari, K.; Trucks, G. W.; Pople, J. A. *J. Chem. Phys.* **1991**, *94*, 7221.
- (10) Friesner, R. A.; Murphy, R. B.; Beachy, M. D., in press.
- (11) Honig, B.; Sharp, K.; Yang, A. *J. Phys. Chem.* **1993**, *97*, 1101.
- (12) Tannor, D.; Marten, B.; Murphy, R.; Ringnalda, M.; Friesner, R. A.; Nicholls, A.; Goddard, W. A., III; Honig, B. *J. Am. Chem. Soc.* **1994**, *116*, 11875.
- (13) Marten, B.; Kim, K.; Cortis, C.; Friesner, R. A.; Murphy, R. B.; Ringnalda, M. N.; Sitkoff, D.; Honig, B. *J. Phys. Chem.* **1996**, *100*, 11775.
- (14) Deisenhofer, J.; Epp, O.; Huber, R.; Michl, H. *Nature* **1985**, *318*, 618.
- (15) Deisenhofer, J.; Michl, H. *Science* **1989**, *245*, 463.
- (16) Curtiss, L. A.; Redfern, P. C.; Raghavachari, K.; Pople, J. A. *J. Chem. Phys.* **1998**, *109*, 42.
- (17) Gill, P. M. W.; Johnson, B. G.; Pople, J. A.; Frisch, M. J. *Chem. Phys. Lett.* **1992**, *197*, 499.
- (18) Bartlett, R. J. *J. Phys. Chem.* **1989**, *93*, 3.
- (19) Blomberg, M. R. A.; Siegbahn, P. E. M.; Babcock, G. T. *J. Am. Chem. Soc.* **1998**, *120*, 8812.
- (20) Zhang, L. Y.; Friesner, R. A. *J. Phys. Chem.* **1995**, *99*, 16479.